International Journal of Ambient Energy

ISSN: (Print) (Online) Journal homepage: https://www.tandfonline.com/loi/taen20

Optimisation of the evaporator of a refrigerator employing hydrocarbon as a refrigerant

I Vinoth Kanna

To cite this article: I Vinoth Kanna (2020) Optimisation of the evaporator of a refrigerator employing hydrocarbon as a refrigerant, International Journal of Ambient Energy, 41:11, 1276-1283, DOI: 10.1080/01430750.2018.1507943

To link to this article: https://doi.org/10.1080/01430750.2018.1507943

Published online: 20 Aug 2018.

INTERNATIONAL JOURNAL OF AMBIENT ENERGY
2020, VOL. 41, NO. 11, 1276–1283
https://doi.org/10.1080/01430750.2018.1507943

Taylor & Francis
Taylor & Francis Group

Optimisation of the evaporator of a refrigerator employing hydrocarbon as a refrigerant

I. Vinoth Kanna

Department of Mechanical Engineering, Vel Tech Rangarajan Dr. Sagunthala R&D Institute of Science and Technology, Chennai, India

ABSTRACT

The refrigeration and air conditioning system is a booming research in the research area. In refrigeration, the scientists focus on the new refrigerant in order to reduce the global warming potential (GWP), high coefficient of performance (COP) and meet zero ozone depletion potential (ODP). Not only the new refrigerant as a solution to attain zero ODP, high COP and at the same time to optimise the design of refrigeration system to meet ODP and COP as a required level. This paper aims to optimise the design of a double refrigerator evaporator for a refrigerator employing non ozone-depleting hydrocarbon refrigerant using brine as a secondary solution with a low GWP. It is done by numerical modelling followed by the parametric modelling using CATIA V5.

ARTICLE HISTORY
Received 2 July 2018
Accepted 20 July 2018

KEYWORDS
ODP; GWP; evaporator; refrigerant; brine and CATIA V5

1. Introduction

Normally we preferred hydrocarbon as a refrigerant. Why hydrocarbon refrigerants? The use of hydro fluorocarbon (HFC) refrigerants like R410A, R134a and R32, which are being used as a replacement for ozone depleting CFCs like R12 and HCFCs like R22, has resulted in an alarming threat to the environment because of their high global warming potential (Devaraj, Yuvarajan, and Vinoth Kanna 2018). The advantages of hydrocarbon refrigerants over HFC refrigerants can be seen from their properties and relative performance in Table 1.

With regard to relative performance of hydrocarbon refrigerants against HFC refrigerants and hydro chloro-fluoro-carbons, hydrocarbon refrigerants provide slightly lower refrigerating capacity but as they provide a higher coefficient of performance (COP), they result in lower power consumption (Vinoth Kanna and Paturu 2018).

2. Hydrocarbon refrigerant blends

Hydrocarbon refrigerants like iso-butane (R600a), butane (R600) and propane (R290) are usually used in mixtures for better performance. Some significant hydrocarbon refrigerant blends are the blends of R290/R600a (68:32) and R290/R600 (79:21) (Vinoth Kanna and Pinky 2018a). These stoichiometric mixtures are non-azeotropic refrigerant mixtures which do not boil or condense over constant temperature and exhibit a slight temperature gradient or temperature glide. If the temperature glide of the refrigerant mixture is less than or equal to 5 K, this effect may be neglected (Vinoth Kanna, Vasudevan, and Subramani 2018).

3. Necessity for optimal design of refrigerant equipment

The evaporator design needs to be optimised to minimise the investment cost of refrigerator systems using alternative refrigerants (Vinoth Kanna, Devaraj, and Subramani 2018). The design of the equipment can be optimised to operate in the predetermined service conditions with the objective of minimising the material usage. This would thus save the material cost of the equipment. This has to be done within the capability of the manufacturing process (extrusion) (Paturu and Vinoth Kanna 2018).

4. Double tube evaporators

Double tube evaporators consist of an outer annulus and an inner concentric tube (Vinoth Kanna and Pinky 2018b). The refrigerant circulates in the outer tube while the secondary (brine) solution circulates in the inner tube. Heat exchange occurs usually in the counter flow mode. Figure 1 shows a schematic diagram of the double tube evaporator (Devaraj et al. 2017).

A double tube evaporator using brine solution like $CaCl_2$ brine solution can provide brine directly from the evaporator for application in cooling appliances like chillers. The tubes are usually made of extruded and annealed copper (Gurudath Nayak and Venkatarathnam 2009). The outer tube is provided a polystyrene foam insulation to prevent heat dissipation into the circuit (Oshuoha 2014).

CONTACT I. Vinoth Kanna vinothkanna.research@gmail.com

Table 1. Properties of hydrocarbon refrigerants.

Refrigerant	Saturated vapour pressure (KPa)	Molar mass (g mol^{-1})	Molar vapour specific heat (J mol^{-1} K^{-1})
R290	584.4	44.096	81.88
R134a	374.6	102.03	94.93
R22	621.5	86.468	66.63
R410a	995.0	72.585	87.27
R32	1011.5	52.024	69.16

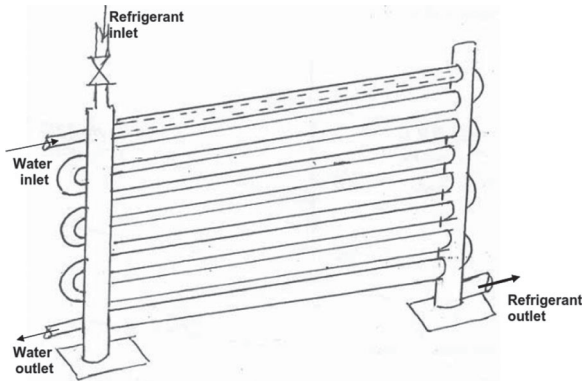

Figure 1. Schematic diagram of a double tube evaporator.

5. Optimal operating conditions for hydrocarbon blends

Experimental investigations by Mani et al. show that the blends of R290/R600a (68:32) and R290/R600 (79:21) provide the best COP under the evaporator operating range (−18°C to 2°C) and load of 0.5 to 2.2 kW (Longo 2012). Iso-butane mixture has a better safety index compared to butane mixtures. Hence the R290/R600a (68:32) mixture can be considered suitable for the retail chillers application (Longo 2010). The brine temperature required at the outlet of the double tube evaporator is selected to be 120°C. The optimum evaporator and condenser temperatures are 2°C and 35°C, respectively. The corresponding pressure in the evaporator and the condenser are $p = 3.9642$ bar and $p = 9.7683$ bar. The inlet temperature of the brine solution is assumed to be 25°C (Alhamid et al. 2013).

If the above-mentioned operating conditions are employed then the cost of the evaporator becomes higher compared to the conventional evaporators. Thus the optimisation of the hydrocarbon evaporator becomes mandatory for the marketing purpose (Longo 2011).

6. Numerical modelling of refrigeration heat exchangers

Work by Nasution et al. (2013) attempted to have a thermo dynamical abstraction of the heat exchange in finned tube evaporators for optimisation. Proceeding on similar lines, the mathematical model of the heat transfer can be developed into a numerical model. This can be taken as an optimisation problem, subject to constraints. The absence of predefined library models of heat transfer with hydrocarbon mixtures involving phase change necessitates the development of a numerical/mathematical model using heat transfer relations (Li and Liu 2016). Regarding hydrocarbon mixtures, limitations in experimental performance data in evaporators of different dimensions make the development of accurate statistical models impractical. (Current data are limited to few models with relation to different operating conditions of the fluid and not the dimensions of the design.)

The numerical model developed based on suitable boiling heat transfer relations could be used as the optimisation problem for the design in relation to the design dimensions. Hence the heat transfer model is developed in relation to the design dimensions as parameters and then optimised for minimisation of material usage. For mathematical models which are used as the basis for refrigeration optimisation, a conformance of 95% of numerical performance predictions with experimental results is desired for validation of the design (Vaitkus and Dagilis 2017).

7. Parametric modelling for design optimisation

The numerical abstraction developed for the optimisation of the design must be related to a parametric model of the evaporator design. Such a model would have the design dimensions of the evaporator as its driving variables. A parametric model thus permits optimisation of design by a metaheuristic search for the design variables/parameters which generate the design model (Özkan and Özil 2006).

The numerical correlations would form the constraints of the parametric model to search for the optimal dimensions. However, the exponential nature of the heat transfer relations for forced convection and boiling heat transfer in the evaporator makes traditional mathematical programming optimisation of the design impractical. Hence the problem must be optimised using metaheuristic search techniques (Yu, Liu, and Zhang 2014).

Furthermore, parametric modelling of the design in a CAD package like CATIA V5 facilitates direct relationship with the numerical abstraction of the model for optimisation. The optimisation of CAD designs involving complicated relations using the native metaheuristic of CATIA V5 is found to be satisfactorily accurate (Clerx and Trezek 1987).

8. Methodology adopted

8.1. Numerical modelling using heat transfer relations

The numerical model of the evaporator is developed using the heat transfer relations corresponding to boiling heat transfer and forced convection heat transfer between the fluids. The relations are derived assuming smooth piping of the evaporator. Flow boiling on the refrigerant side and forced convection heat transfer on the brine side has been assumed (Woo, O'Neal, and Pecht 2010). The complications of the model, namely absence of built-in library models in software packages for the heat transfer in hydrocarbon mixtures involving phase change makes numerical modelling by heat transfer relations the only practical alternative (Tahat, Ibrahim, and Probert 2001).

The relations are substituted for a small concentric cylinder element of length dx and then integrated over the entire length using sufficient assumptions of mean/linear variation. This would result in a logarithmic/exponential equation as the heat transfer relation.

8.2. Optimisation of design using a metaheuristic search

The heat transfer relation is complicated involving a logarithmic/exponential function which forms one of the constraints of the optimisation problem. Hence it would be impractical to solve it by traditional mathematical programming techniques. So it would be practical to solve the design optimisation using a metaheuristic algorithm like simulated annealing (SA). The inaccuracy of the method would be negligible compared to the manufacturing tolerance of the manufacturing method (Björk and Palm 2008).

9. Parametric modelling of the design using CATIA V5

The parametric model of the double tube evaporator can be developed in CATIA V5 directly in relation to the principal design dimensions, namely outer diameter of outer and inner tubes, thickness of the tubes and the total tube length. This is done so as to generate the entire design based on these variables.

Parametric modelling in CATIA V5 facilitates direct optimisation of the model as there is a native SA metaheuristic macro in the Product Engineering Optimizer (PEO) workbench of CATIA V5. This allows the parametric model to be associated with the numerical abstraction of the heat transfer model through the problem definition module of the workbench.

Among the metaheuristic search procedures available, the SA metaheuristic procedure is preferred as it facilitates continuous search for the design variables within the search space for a design problem. It searches in a pattern accepting solutions giving continuous improvement or solutions which provide slight decrement, based on a probability.

$$\text{Probability (acceptance)} = e^{\left(\frac{Z_c - Z_n}{T}\right)}$$

where Z_c is the current trial solution, Z_n is the next trial solution and T is the parameter which is a product of temperature in the current contour and Boltzmann constant.

If the random number generated is greater than probability function, the current solution is accepted. The native metaheuristic algorithm, i.e. SA, will offer very accurate results in the case of parametrically modelled CAD models.

To optimise the design using the native SA algorithm, the design problem and its heat transfer constraint must be adapted into an acceptable form of functions, which can be manipulated by the SA macro iteratively. The final design is generated as a parametric model of the optimal solution of the SA run.

10. Heat transfer conditions and assumptions

The thermal and physical properties of the refrigerant mixture were obtained from REFPROP database, NIST Reference. The dimensions of the initial double tube section, present in the existing test rig, are

- D0 = 15.87 mm
- Di = 14.45mm
- d0 = 9.52 mm
- di = 8.10 mm

Mean variation is assumed for the properties along the evaporation line. For a standard mass flow rate of 8.67×10^{-3} kg/s for the refrigerant mixture the velocity of flow of the refrigerant in the initial tube section was calculated and Reynold's number was calculated for bulk mean conditions as Re = 13,292. Hence it is a turbulent flow (Re > 2300).

For a standard mass flow rate of 0.0725 kg/s for brine, Reynold's number has been estimated to be Re = 932. Hence it is a laminar flow (Re < 2300).

The evaporating condition has been equated to the flow boiling of a refrigerant mixture because the refrigerant is flowing continuously in tubes and not in a shell; hence there is not adequate surface area for nucleate pool boiling to take place.

Among all correlations for flow boiling, the Bo Pierre's correlation for average Nusselt's number has been chosen (Refrigeration Handbook, IIT-Kharagpur, 2008). Bo Pierre's correlation gives average heat transfer coefficient for forced convection boiling. The average Nusselt's number is given by

$$N_u = 0.0082\sqrt{R_e{}^2 k}$$

where

$$k = \frac{\mathrm{d}X h_{fg}}{l}$$

dX is the change in dryness fraction, h_{fg} is the latent heat of vaporisation = 365.87 kJ/kg and l is the length (m)

The flow of brine solution is laminar and hence Nusselt's number Nu is independent of Reynold's number. The heat transfer by forced convection is expressed by Nusselt's number as $N_u = 3.66$ (constant).

11. Heat transfer relations for the small cylinder of the tube

The energy equation for the small tube element as shown in Figure 2 of length dx in counter flow mode is

$$Q_{Conv} = Q_{Cond}$$

i.e.

$$\frac{t_{br} - t_{evap}}{(1/h_{br} \times \pi \times d_i \times \mathrm{d}x)} + \frac{\ln(d_0/d_i)}{(k_{copper} \times 2\pi \times \mathrm{d}x)} + \frac{1}{h_{ref} \times \pi \times d_0 \times \mathrm{d}x} = m_{br} \times C_{pbr} \times \frac{\mathrm{d}t_b}{\mathrm{d}x} \times \mathrm{d}x = h_{fg} \times m_{ref} \times \frac{\mathrm{d}X}{\mathrm{d}x} \times \mathrm{d}x \quad (1)$$

where Q_{Conv} is the convective heat transfer (kJ), Q_{Cond} is the conductive heat transfer (kJ), t_{br} is the temperature of brine (°C), t_{evap}

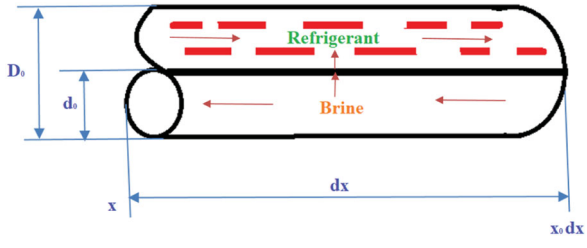

Figure 2. A small cylinder of the double tube.

is the temperature of refrigerant mixture (°C), h_{br} is the mean convective heat transfer coefficient of brine (W/m^{2}K), h_{ref} is the mean convective heat transfer coefficient of refrigerant mixture (W/m^{2}K), k_{copper} is the convective heat transfer (kJ), m_{br} is the mass flow rate of brine (kg/s) and m_{ref} is the mass flow rate of refrigerant mixture (kg/s).

Now the heat transfer coefficients are given by

$$h = N_u \times \frac{k}{d}$$

We have $X = 0.234$ at $x = 0$, $X = 1$ at $x = \mathrm{L}$, $t_{br} = 25$°C at $x = \mathrm{L}$ and $t_{br} = 12$°C at $x = 0$ as the boundary conditions.

Substituting corresponding values in the differential Equation (1), we have

$$\frac{t_{br} - 2}{((1/5.736) + \ln((d_0/d_i)/2425.31))} + (D_i^2 - d_0^2) \times L^{(0.5/3.185 d_0)} = 3.1709 \times 10^3 \times \mathrm{d}x = 0.055 \times 2782 \times (\mathrm{d}t_{br}/\mathrm{d}x) \quad (2)$$

12. Integration and constraint derivation

Integrating the above Equation (2) within the given boundaries and solving we have:

$$t_{br} = \frac{23}{e^{\left(\frac{L}{0.055\times 2782} \times \left(\frac{1}{5.736} + \frac{\ln(d_0/d_i)}{2425.31}\right) + \left(\frac{D_i^2 - d_0^2}{3.185 \times L^{0.5/d_0}}\right)\right)}} + 2 \quad (3)$$

and

$$Q_{\max} = 0.055 \times 2782 \times \left(1 - e^{\left(\frac{L}{0.055\times 2782} \times \left(\frac{1}{5.736} + \frac{\ln(d_0/d_i)}{2425.31}\right) + \left(\frac{D_i^2 - d_0^2}{3.185 \times L^{0.5/d_0}}\right)\right)}\right) \quad (4)$$

The above (Equations (3) and (4)) relations give the abstraction of the heat transfer relations in the evaporator. Using these as constraints, the problem for design optimisation is defined.

Objective: To minimise the material volume of the design subject to,

$$t_{br}\ (\text{at } x = 0) = \frac{23}{e^{\left(\frac{L}{0.055\times 2782} \times \left(\frac{1}{5.736} + \frac{\ln(d_0/d_i)}{2425.31}\right) + \left(\frac{D_i^2 - d_0^2}{3.185 \times L^{0.5/d_0}}\right)\right)}} + 2 = 12^{\circ}\mathrm{C} \quad (5)$$

$$Q_{\max} = 0.055 \times 2782 \times \left(1 - e^{\left(\frac{L}{0.055\times 2782} \times \left(\frac{1}{5.736} + \frac{\ln(d_0/d_i)}{2425.31}\right) + \left(\frac{D_i^2 - d_0^2}{3.185 \times L^{0.5/d_0}}\right)\right)}\right) = 2.49\ \mathrm{kW} \quad (6)$$

$$\frac{D_0 - d_i}{2} \text{ and } \frac{d_0 - d_i}{2} = 0.35\ \text{mm or 29SWG} \times (\text{manufacturing constraints for extrusion or tube drawing}) \quad (7)$$

$$\text{Hoop's stress in the tubes (due to pressure)} = P_{\text{evap}} \times \frac{d_i}{d_0 - d_i} = 0.3964 \times \frac{d_i}{d_0 - \mathrm{d}_i} = 650\ \text{bar (65Mpa)} \quad (8)$$

and

$$P_{\text{evap}} \times \frac{D_i - d_0}{D_0 - D_i} = 0.3964 \frac{D_i - d_0}{D_0 - D_i} = 650\ \text{bar (65MPa)}$$

where P_{evap} is the evaporator pressure $= 3.9642$ bar.

13. Parametric modelling of the evaporator

13.1. Initial design model of evaporator in CATIA V5

Parametric modelling of the double tube assembly is done so that the optimisation procedure can drive the generation of the model via knowledge ware of CATIA V5. Successive update

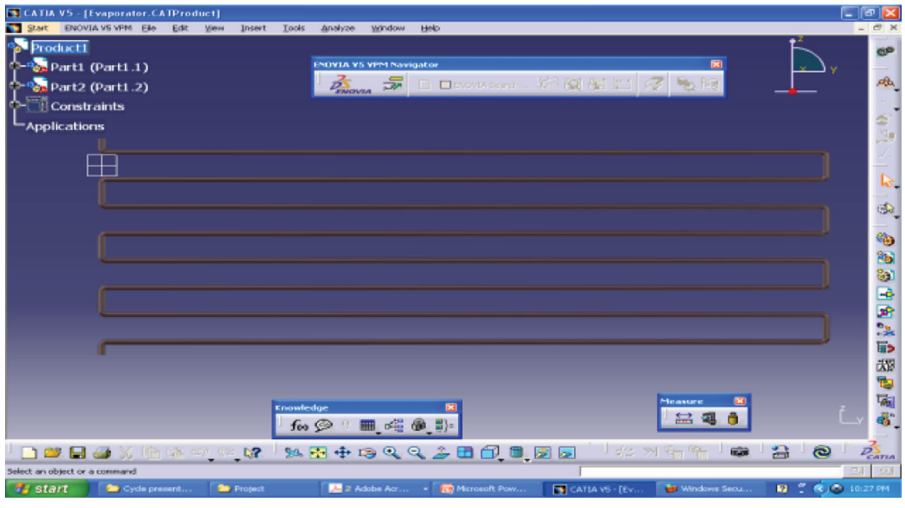

Figure 3. Initial parametric model in CATIA V5.

of the model can be achieved using the parametric modelling approach.

The free variables namely siameters, thickness, length, number of coils (in terms of double runs) can drive the entire model to evaluate the objective function for each trial. Properties of copper for the tube are imported from CATIA's material library. The initial dimensions of tube diameters, length, etc. are used as such as in the existing model (Figure 3).

14. Optimisation of the design

14.1. Problem definition in the PEO workbench

The problem was defined in the PEO workbench of CATIA V5 with the objective of minimisation of material volume of the model (and hence the amount of metal). The problem and the independent variables, namely the design dimensions are defined (Figure 4).

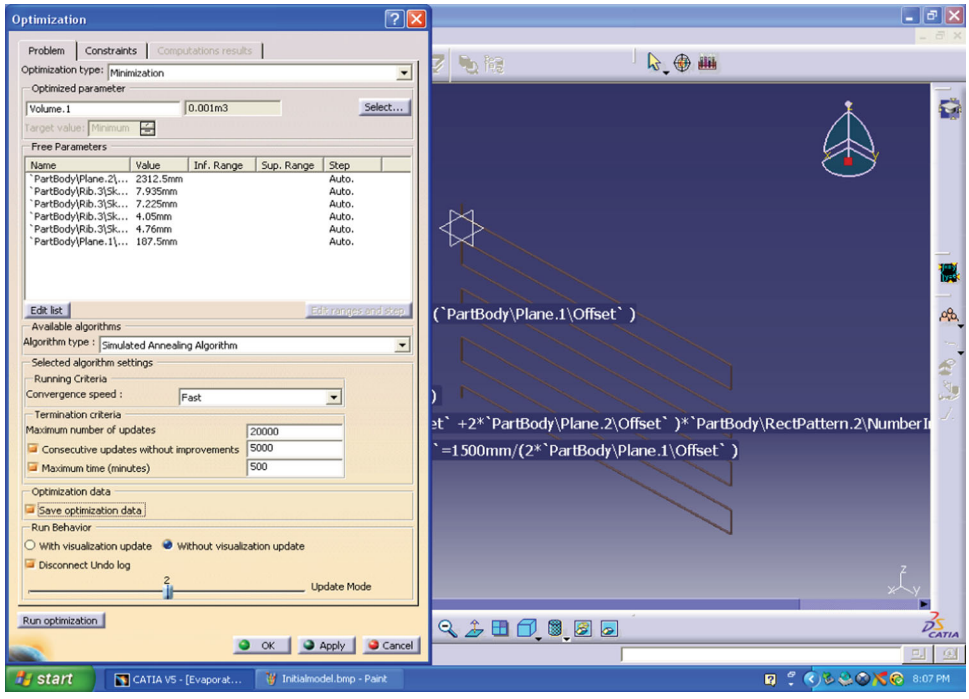

Figure 4. Problem definition with the initial model.

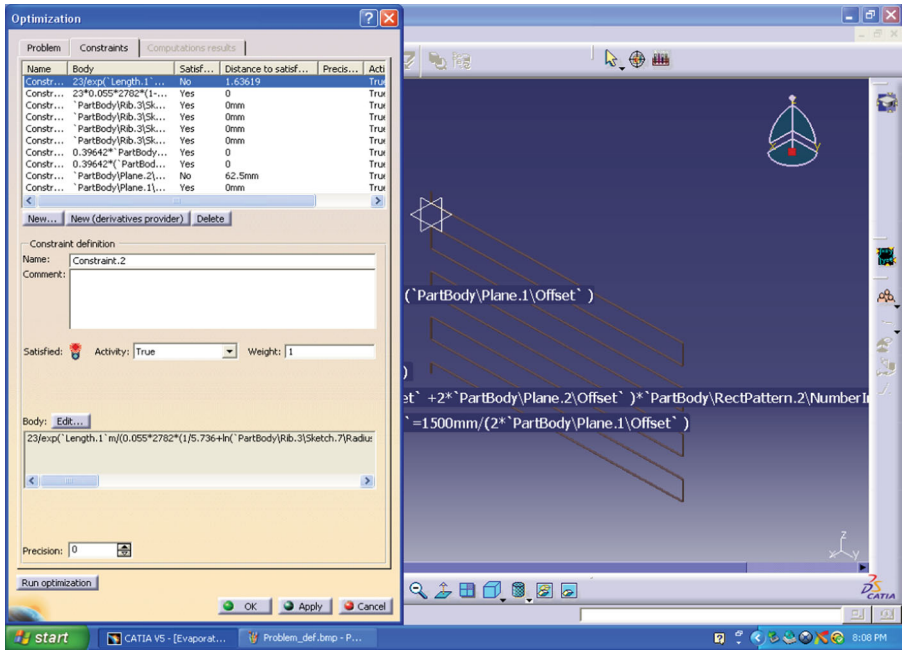

Figure 5. Definition of the constraints for the optimisation problem.

15. Constraint definition in the PEO workbench

The constraints derived in the previous chapter are defined in the PEO workbench of CATIA V5 (Figure 5).

It must be noted that the geometrical layout of the evaporator is not rigidly fixed. The design optimisation is focused only on the dimensions of the tube. The geometric design is decided based only on practical considerations to reduce the pressure drop.

16. Staging the SA run

Since the SA inbuilt algorithm is being used to solve a design problem involving a vast search space, the number of iterations in the algorithm is very high (total of approximately 90,000). Hence the search space is divided into domains with varying number of trials, convergence intervals and cooling times. The convergence requirements were varied from domain to domain, i.e. narrower intervals and greater trials for small intervals, more time, etc. as the search space contracted and the solution grew closer to the global optimum.

This was done to ensure that the algorithm did not prematurely converge into a random local optimum. This is analogous to the natural process of visual searching for features on topography, by the human eye. A similar approach using a general search followed by deep probes into the search space was suggested by Puaro et al. for multi-objective decision-making.

The search domain categorisation based on the material volume range/function and the respective search time for each stage is described below:

- Run 1: 27000 trials, cooling time = 530 minutes; Search space (0.000637855 m^3, 0.000612996 m^3)

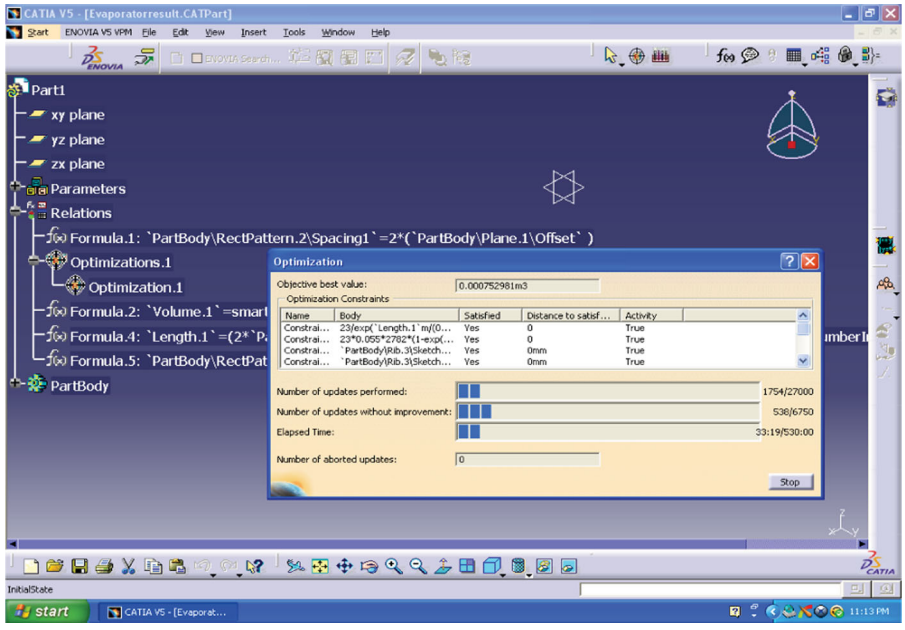

Figure 6. The first run of the SA search.

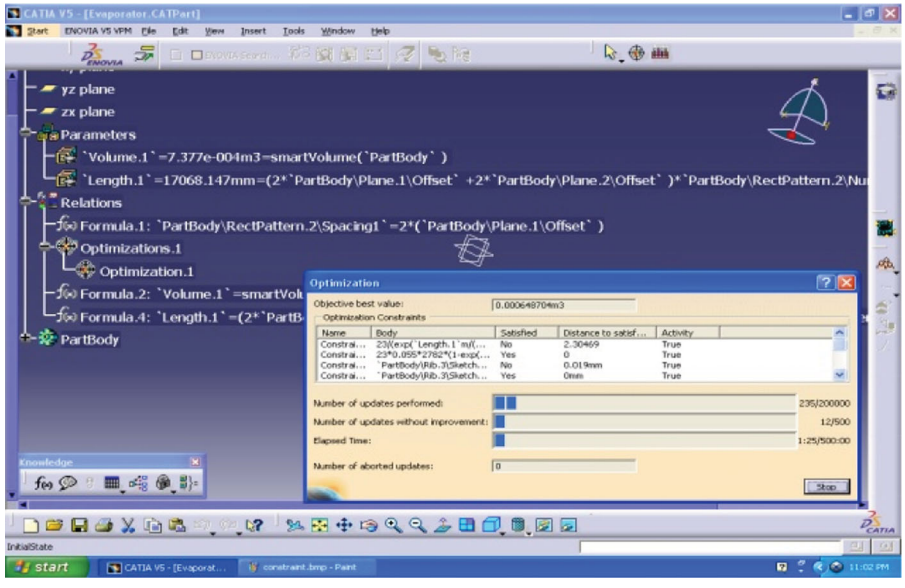

Figure 7. The third run of the SA search.

- Run 2: 5963 trials, cooling time = 100 minutes; Search space (0.000612996 m^3, 0.000612621 m^3)
- Run 3: 20000 trials, cooling time = 500 minutes; (but only 19914 could be generated) Search space (0.000612621 m^3, 0.000527156 m^3)
- Run 4: 20000 trials, cooling time = 500 minutes; Search space (0.000527156 m^3, 0.000557275 m^3).
- Run 5: 20000 trials, cooling time = 500 minutes; Search space (0.000557275 m^3, 0.000561195 m^3)

17. Results of the metaheuristic search

The SA metaheuristic was executed in stages as described earlier. The SA execution is illustrated (Figures 6–7).

18. Material saving achieved in the optimised design

The optimised design generated by the SA metaheuristic search has the following changes from the initial design:

> The optimised length has an increased length (from 15 to 23.575 m) (including the bends) and reduced wall thickness (from 0.71 mm or 22 SWG to 0.35 mm or 29 SWG)
> Hence there is a reduction in material volume (from 0.000637855 to 0.000561195 m^3 (or 12% material reduction).

This would give a material savings of 0.685 kg of copper (density = 8940 kg/m^3) in the evaporator tube.

However, the optimisation of the design was concerned with the overall dimensions of the evaporator. It must be noted that the geometrical design has 28 horizontal rows and hence there would be a significant pressure drop. Hence the geometry is altered during installation, but would be independent of the overall dimensions as it is a flexible tube (Figure 8).

Figure 8. Optimised evaporator.

19. Conclusion

The variables controlling the design of the evaporator are determined by numerical modelling and these variables are parametrically modelled to obtain the optimised design of the evaporator.

ORCID

I. Vinoth Kanna http://orcid.org/0000-0001-8194-8781

References

Alhamid, M. I., Nasruddin, R.B.S., Darwin, and ArnasLubis. 2013. "Characteristics and COP Cascade Refrigeration System using Hydrocarbon Refrigerant (Propane, Ethane and CO2) at Low Temperature Circuit (TC)." *International Journal of Technology* 4 (2): 112. doi:10.14716/ijtech.v4i2.125.

Björk, E., and B. Palm. 2008. "Flow Boiling Heat Transfer at Low Flux Conditions in a Domestic Refrigerator Evaporator." *International Journal of Refrigeration* 31 (6): 1021–1032. doi:10.1016/j.ijrefrig.2007.12.017.

Clerx, M., and G. J. Trezek. 1987. "Performance of an Aqua-Ammonia Absorption Solar Refrigerator at Sub-Freezing Evaporator Conditions." *Solar Energy* 39 (5): 379–389. doi:10.1016/s0038-092x(87)80056-7.

Devaraj, A., I. Vinoth Kanna, K. Manikandan, and Jishuchandran. 2017. "Impact of Engine Emissions from HCCI Engine, an Overview." *International Journal of Mechanical and Production Engineering Research and Development* 7 (6): 501–506. doi:10.24247/ijmperddec201757.

Devaraj, A., D. Yuvarajan, and I. Vinoth Kanna. 2018. "Study on Outcome of Cetane Improver on Emission Characteristics of a Diesel Engine." *International Journal of Ambient Energy* 1–9. doi:10.1080/01430750.2018.1492452.

Gurudath Nayak, H., and G. Venkatarathnam. 2009. "Performance of an Auto Refrigerant Cascade Refrigerator Operating in Gas Refrigerant Supply (GRS) Mode with Nitrogen–Hydrocarbon and Argon–Hydrocarbon Refrigerants." *Cryogenics* 49 (7): 350–359. doi:10.1016/j.cryogenics.2009.04.002.

Li, H., and Y. Liu. 2016. "Numerical Investigation of Boiling Heat Transfer on Hydrocarbon Mixture Refrigerant in Vertical Rectangular Minichannel." *Advances in Mechanical Engineering* 8 (6). doi:10.1177/1687814016651818.

Longo, G. A. 2010. "Heat Transfer and Pressure Drop During Hydrocarbon Refrigerant Condensation Inside a Brazed Plate Heat Exchanger." *International Journal of Refrigeration* 33 (5): 944–953. doi:10.1016/j.ijrefrig.2010.02.007.

Longo, G. A. 2011. "The Effect of Vapour Super-Heating on Hydrocarbon Refrigerant Condensation Inside a Brazed Plate Heat Exchanger." *Experimental Thermal and Fluid Science* 35 (6): 978–985. doi:10.1016/j.expthermflusci.2011.01.018.

Longo, G. A. 2012. "Hydrocarbon Refrigerant Vaporization Inside a Brazed Plate Heat Exchanger." *Journal of Heat Transfer* 134 (10): 101801. doi:10.1115/1.4006817.

Nasution, H., Zulkarnain Abdul Latiff, Azhar Abdul Aziz, Mohd Rozi Mohd Perang. 2013. "Retrofitting R-22 Split Type Air Conditioning with Hydrocarbon (HCR-22) Refrigerant." *Applied Mechanics and Materials* 388: 91–95. doi:10.4028/www.scientific.net/amm.388.91.

Oshuoha, I. C. 2014. "Hydrocarbon-Butane an Alternative Refrigerant for CFCS and HCFCS." *IOSR Journal of Engineering* 4 (5): 34–37. doi:10.9790/3021-04573437.

Özkan, D. B., and E. Özil. 2006. "Experimental Study on the Effect of Frost Parameters on Domestic Refrigerator Finned Tube Evaporator Coils." *Applied Thermal Engineering* 26 (17-18): 2490–2493. doi:10.1016/j.applthermaleng.2006.04.015.

Paturu, P., and I. Vinoth kanna. 2018. "Experimental Investigation of Performance and Emissions Characteristics on Single Cylinder Direct Injection Diesel Engine with PSZ Coating Using Radish Biodiesel." *International Journal of Ambient Energy* 1–19. doi:10.1080/01430750.2018.1492455.

Tahat, M. A., G. A. Ibrahim, and S. D. Probert. 2001. "Performance Instability of a Refrigerator with Its Evaporator Controlled by a Thermostatic Expansion-Valve." *Applied Energy* 70 (3): 233–249. doi:10.1016/s0306-2619(01)00034-4.

Vaitkus, L., and V. Dagilis. 2017. "Experimental Investigation of Transport Refrigerator with Eutectic Plate Evaporator and Economizer with Intermediate Heat Exchanger." *Mechanics* 23 (1). doi:10.5755/j01.mech.23.1.14319.

Vinoth Kanna, I., A. Devaraj, and K. Subramani. 2018. "Bio Diesel Production by Using Jatropha: The Fuel for Future." *International Journal of Ambient Energy* 1–7. doi:10.1080/01430750.2018.1456962.

Vinoth Kanna, I., and P. Paturu. 2018. "A Study of Hydrogen as an Alternative Fuel." *International Journal of Ambient Energy* 1–4. doi:10.1080/01430750.2018.1484803.

Vinoth Kanna, I., and D. Pinky. 2018a. "Automatic Sea Level Control Using MEMS Programmed with Lab VIEW." *International Journal of Ambient Energy* 1–4. doi:10.1080/01430750.2018.1484813.

Vinoth Kanna, I., and D. Pinky. 2018b. "Solar Research – A Review and Recommendations for the Most Important Supplier of Energy for the Earth with Solar Systems." *International Journal of Ambient Energy* 1–7. doi:10.1080/01430750.2018.1472658.

Vinoth Kanna, I., A. Vasudevan, and K. Subramani. 2018. "Internal Combustion Engine Efficiency Enhancer by Using Hydrogen." *International Journal of Ambient Energy* 1–4. doi:10.1080/01430750.2018.1456961.

Woo, S., D. L. O'Neal, and M. Pecht. 2010. "Failure Analysis and Redesign of the Evaporator Tubing in a Kimchi Refrigerator." *Engineering Failure Analysis* 17 (2): 369–379. doi:10.1016/j.engfailanal.2009.08.003.

Yu, Q., J. Liu, and K. Zhang. 2014. "The Computer Aided Fault Tree Modeling and Analysis of the Refrigerator Evaporator Failure." *The Open Mechanical Engineering Journal* 8 (1): 26–30. doi:10.2174/1874155x01408010026.